Supplement of Atmos. Chem. Phys., 25, 997–1021, 2025
https://doi.org/10.5194/acp-25-997-2025-supplement
© Author(s) 2025. CC BY 4.0 License.

Atmospheric Chemistry and Physics
Open Access

Supplement of

Solar radiation estimation in West Africa: impact of dust conditions during the 2021 dry season

Léo Clauzel et al.

Correspondence to: Léo Clauzel (leo.clauzel@univ-grenoble-alpes.fr) and Sandrine Anquetin (sandrine.anquetin@univ-grenoble-alpes.fr)

The copyright of individual parts of the supplement might differ from the article licence.

Supplementary materials

Several metrics are used to assess the quality of the simulations such as the Mean Absolute Error (MAE, eq. S1), the normalised Mean Absolute Error ($nMAE$, eq. S2), the Mean Bias Error (MBE, eq. S3) the Pearson correlation coefficient ($corrcoef$, eq. S4) and the Index of Agreement (IOA, eq. S5, Legates and McCabe, 2013) :

$$MAE = \frac{1}{N}\sum_{i=1}^{N}\left|f_i - o_i\right| \quad \text{(eq. S1)}$$

$$nMAE = \frac{100 * MAE}{max\left(o_i\right)} \quad \text{(eq. S2)}$$

$$MBE = \frac{1}{N}\sum_{i=1}^{N}\left(f_i - o_i\right) \quad \text{(eq. S3)}$$

$$corrcoef = \frac{\sum_{i=1}^{N}\left(o_i - \bar{o}\right)\left(f_i - \bar{f}\right)}{\sqrt{\sum_{i=1}^{N}\left(o_i - \bar{o}\right)^2}\sqrt{\sum_{i=1}^{N}\left(f_i - \bar{f}\right)^2}} \quad \text{(eq. S4)}$$

$$IOA = 1 - \frac{\sum_{i=1}^{N}\left|f_i - o_i\right|}{\sum_{i=1}^{N}\left(\left|f_i - \bar{o}\right| + \left|o_i - \bar{o}\right|\right)} \quad \text{(eq. S5)}$$

where o refers to the observations and f to the forecasts. The MAE gives equal weight to all errors and is less sensitive to outliers. $nMAE$ enables the comparison of errors in data with varying amplitudes. MBE is used to estimate the average bias of the simulations. Lower values of MAE, $nMAE$ and MBE indicate a better model accuracy. The Pearson correlation coefficient $corrcoef$ measures the linear correlation between two variables. A higher absolute value of $corrcoef$ suggests a stronger linear correlation. The IOA is a standardised measure that detects additive and proportional differences in the observed and simulated means and variances, providing a measure of the degree of model errors. An agreement value of 1 indicates a perfect match, while 0 indicates no agreement at all.

Table S1 - Dust refraction indices (real and imaginary part) for the computation of dust radiative properties given in CHIMERE model (Menut et al., 2021 ; Kandler et al., 2007).

$\lambda(nm)$	$\Re(n)$	$\Im(n)$
200	1.53	5.5×10^{-3}
300	1.53	5.5×10^{-3}
400	1.53	2.4×10^{-3}
600	1.53	8.9×10^{-4}
999	1.53	7.6×10^{-4}

Table S2 - Dust aerosol radiative properties for the 10 CHIMERE aerosol size bins (Mie theory calculation). r_{eff} is the effective radius (in µm), Q is the extinction coefficient, SSA is the single-scattering albedo and $\omega_{1\le i\le 7}$ are the first 7 terms of the Taylor expansion of the scattering phase function.

$\lambda(nm)$	r_{eff}	Q	SSA	ω_1	ω_2	ω_3	ω_4	ω_5	ω_6	ω_7
Dust 1										
200	0.098	3.7320	0.9763	2.194	2.688	2.482	1.887	1.217	0.611	0.181
300	0.098	2.1717	0.9751	1.947	1.789	1.067	0.482	0.123	0.024	0.004
400	0.098	1.1436	0.9858	1.708	1.146	0.393	0.106	0.018	0.002	0.000
600	0.098	0.3239	0.9911	0.823	0.627	0.148	0.018	0.001	0.000	0.000
999	0.098	0.0501	0.9764	0.283	0.515	0.052	0.002	0.000	0.000	0.000
Dust 2										
200	0.149	3.7097	0.9632	2.104	2.860	2.897	3.010	2.862	2.552	2.146
300	0.149	3.8024	0.9767	2.195	2.692	2.454	1.814	1.112	0.532	0.129
400	0.149	2.6412	0.9896	2.019	2.042	1.405	0.688	0.187	0.043	0.007
600	0.149	1.0626	0.9945	1.692	1.080	0.353	0.086	0.013	0.001	0.000
999	0.149	0.2111	0.9902	0.590	0.564	0.106	0.010	0.001	0.000	0.000
Dust 3										
200	0.210	2.1345	0.9092	1.596	2.133	1.578	1.994	1.824	2.131	2.247
300	0.210	3.9009	0.9666	2.148	2.899	2.956	2.969	2.727	2.267	1.743
400	0.210	3.9485	0.9895	2.199	2.757	2.609	2.066	1.394	0.712	0.210
600	0.210	2.3853	0.9960	1.955	1.864	1.152	0.532	0.136	0.027.	0.004
999	0.210	0.6475	0.9944	1.300	0.814	0.240	0.044	0.005	0.000	0.000
Dust 4										
200	0.319	2.5556	0.8925	2.270	3.369	3.761	4.635	4.785	5.321	5.282
300	0.319	2.1960	0.9092	1.668	2.279	1.838	2.320	2.171	2.501	2.523

400	0.319	3.2922	0.9795	1.979	2.684	2.583	2.754	2.637	2.494	2.285
600	0.319	3.9629	0.9959	2.186	2.767	2.630	2.156	1.529	0.878	0.368
999	0.319	2.0516	0.9965	1.902	1.677	0.915	0.394	0.096	0.0018	0.002
Dust 5										
200	0.493	2.3054	0.8513	2.348	3.416	3.827	4.710	5.112	5.940	6.348
300	0.493	2.5953	0.8929	2.308	3.427	3.866	4.744	4.917	5.454	5.440
400	0.493	2.1819	0.9516	1.772	2.579	2.321	3.101	2.976	3.461	3.335
600	0.493	3.2132	0.9919	1.942	2.640	2.511	2.720	2.639	2.565	2.416
999	0.493	3.8226	0.9967	2.185	2.680	2.455	1.835	1.148	0.559	0.141
Dust 6										
200	0.740	2.2360	0.8042	2.468	3.652	4.293	5.309	5.916	6.898	7.500
300	0.740	2.3054	0.8513	2.348	3.416	3.827	4.710	5.112	5.940	6.348
400	0.740	2.3952	0.9387	2.246	3.260	3.478	4.195	4.192	4.693	4.664
600	0.740	2.1753	0.9814	1.743	2.548	2.247	3.033	2.875	3.368	3.226
999	0.740	3.6805	0.9946	2.059	2.801	2.789	2.883	2.713	2.402	2.034
Dust 7										
200	1.110	2.1857	0.7495	2.569	3.858	4.727	5.865	6.735	7.882	8.748
300	1.110	2.2360	0.8042	2.468	3.652	4.293	5.309	5.916	6.898	7.500
400	1.110	2.2944	0.9186	2.297	3.379	3.695	4.645	4.948	5.820	6.124
600	1.110	2.3941	0.9752	2.207	3.211	3.365	4.083	4.025	4.531	4.466
999	1.110	2.0755	0.9851	1.562	2.172	1.571	2.123	1.865	2.256	2.223
Dust 8										
200	1.654	2.1364	0.6889	2.657	4.059	5.165	6.427	7.555	8.848	9.972
300	1.654	2.1891	0.7509	2.568	3.856	4.722	5.859	6.726	7.871	8.735
400	1.654	2.2338	0.8903	2.401	3.552	4.017	5.023	5.482	6.490	6.998
600	1.654	2.2906	0.9666	2.247	3.311	3.526	4.468	4.678	5.547	5.782
999	1.654	2.6197	0.9823	2.219	3.316	3.603	4.482	4.524	5.079	4.986
Dust 9										
200	2.466	2.1087	0.6323	2.736	4.273	5.630	7.055	8.436	9.888	11.257
300	2.466	2.1359	0.6895	2.656	4.056	5.158	6.419	7.542	8.834	9.953
400	2.466	2.1796	0.8520	2.480	3.693	4.303	5.373	6.006	7.126	7.815
600	2.466	2.2386	0.9541	2.338	3.463	3.792	4.789	5.113	6.112	6.505
999	2.466	2.3090	0.9723	2.222	3.248	3.416	4.291	4.467	5.291	5.539
Dust 10										
200	3.915	2.0781	0.5812	2.801	4.490	6.092	7.706	9.317	10.939	12.530
300	3.915	2.1031	0.6236	2.746	4.306	5.701	7.154	8.571	10.049	11.452

400	3.915	2.1224	0.7926	2.565	3.854	4.658	5.801	6.653	7.879	8.785
600	3.915	2.1676	0.9321	2.410	3.585	4.010	5.053	5.504	6.612	7.155
999	3.915	2.2181	0.9614	2.319	3.430	3.722	4.7000	4.977	5.945	6.289

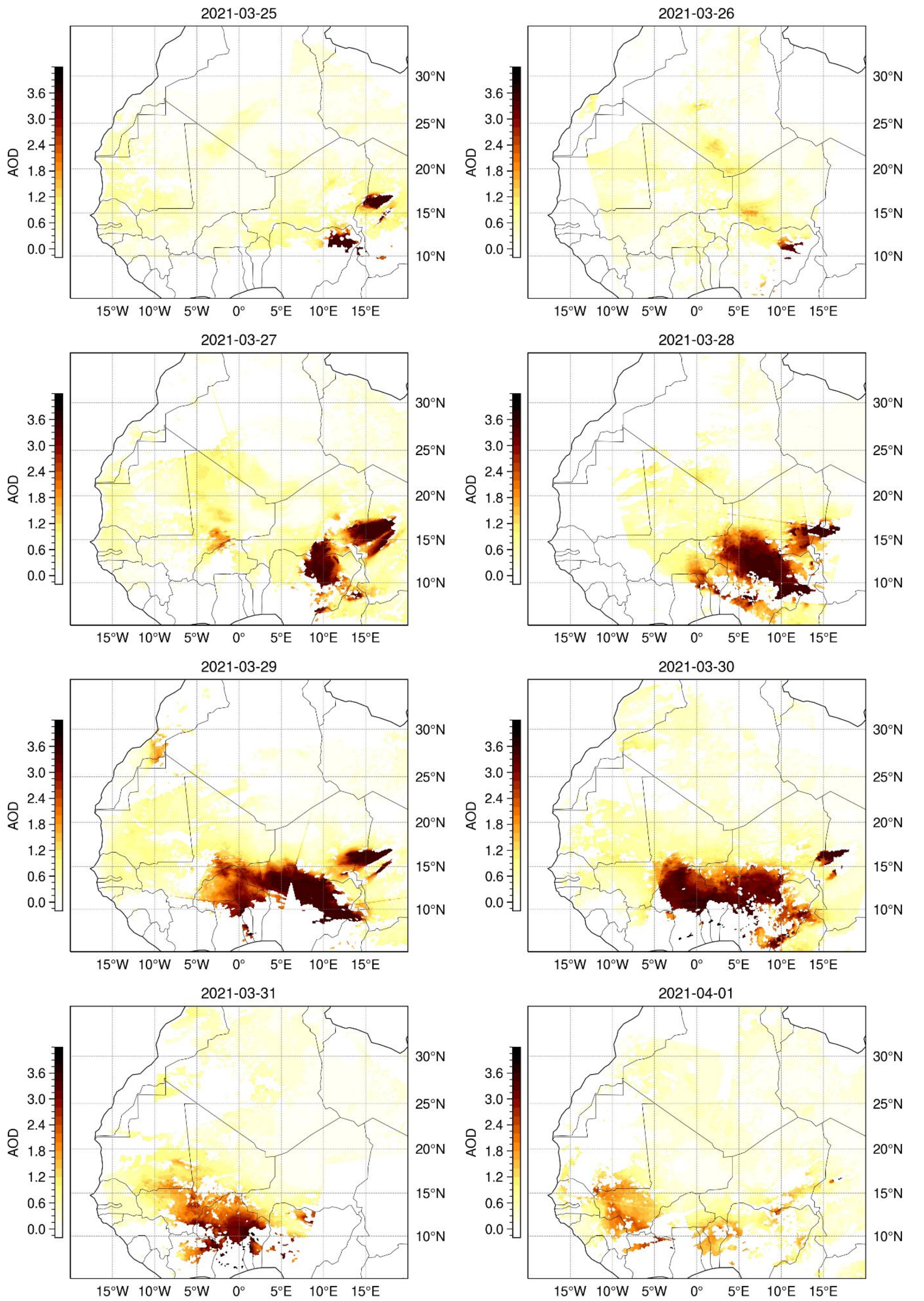

Figure S1 - Daily mean Aerosol Optical Depth at 550nm from MODIS satellite observations from 25 March to 01 April 2021.

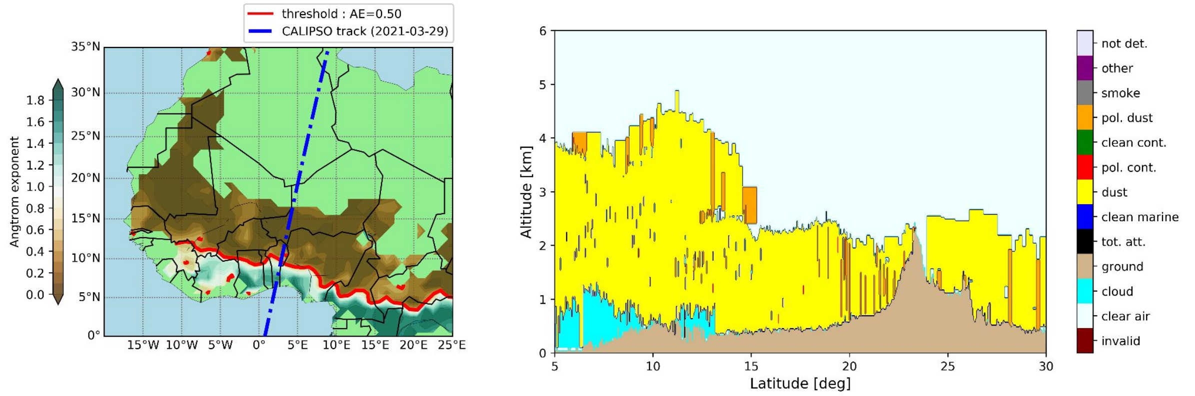

Figure S2 - The left panel displays the MODIS level 3 Ångström Exponent averaged over the case study period (28 March to 01 April 2021) for MODIS AOD values greater than 0.5. The blue dashed lines represent the CALIPSO satellite track on 29 March 2021. The right panel shows the CALIOP Vertical Feature Mask (VFM) from the CALIPSO satellite overpass on 29 March 2021.

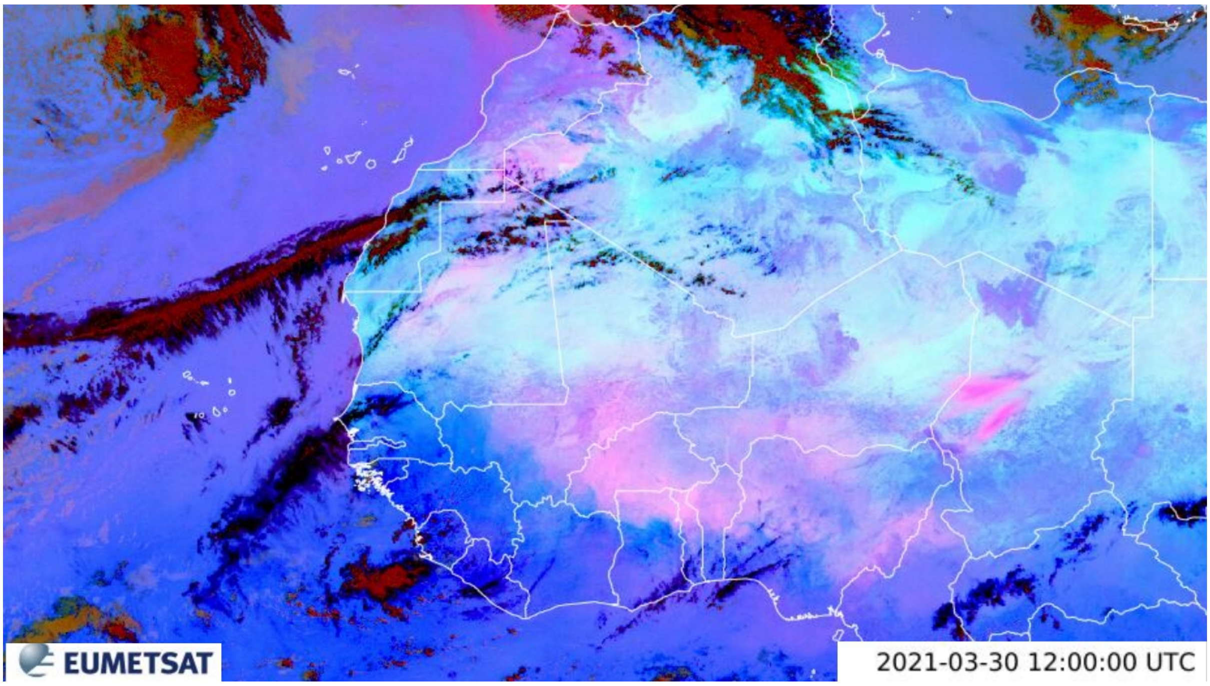

Figure S3 - MSG Dust RGB composite on 30 March 2021 at 12h. Pink areas correspond to dust plums, black areas are cirrus clouds with no clouds below, red refers to thick, high and cold ice clouds.

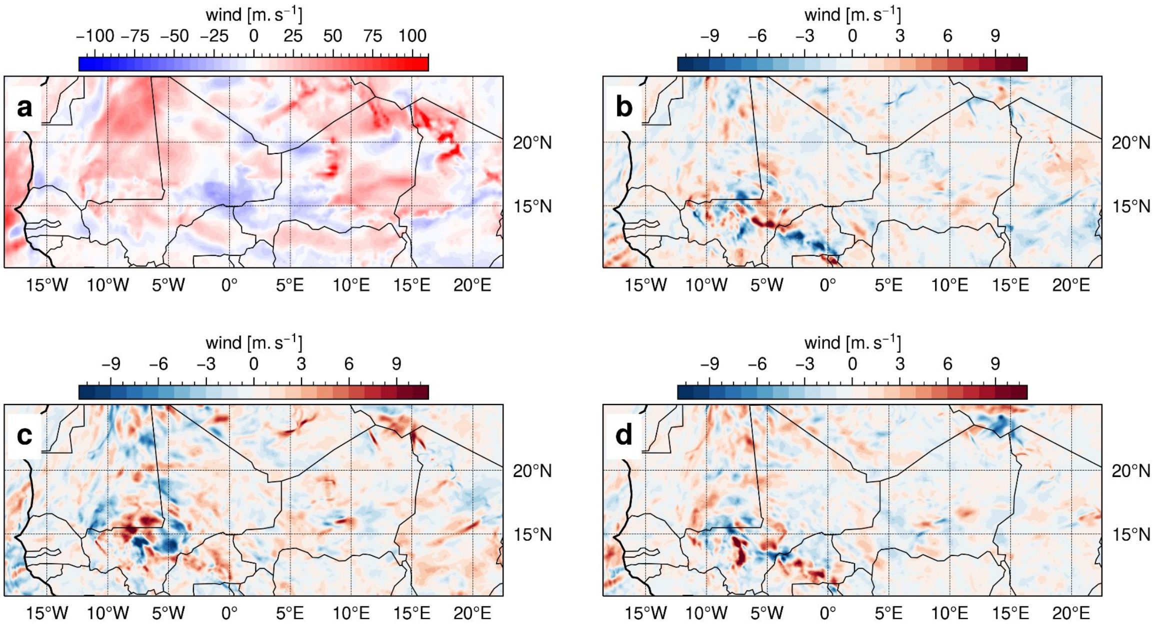

Figure S4 - Squared surface wind speed on March 28th at 10h with a) the difference between the three WRF-CHIMERE simulation average and ERA5 reanalysis. For panels b, c and d, squared surface wind speed on March 28th at 10h differences between each of the WRF-CHIMERE simulations driven by GOCART, MERRA2 and CAMS, respectively, and the mean of the three WRF-CHIMERE simulations. The time used for the figure was selected since it corresponds to the maximum of dust emission flux during case study. The surface wind speed is squared, given that dust emissions are determined by wind velocities with a squared velocity.